Cell Stress and Chaperones (2015) 20:37–46
DOI 10.1007/s12192-014-0523-6

ORIGINAL PAPER

Upregulation of heat shock proteins and the promotion of damage-associated molecular pattern signals in a colorectal cancer model by modulated electrohyperthermia

Gabor Andocs · Nora Meggyeshazi · Lajos Balogh · Sandor Spisak · Mate Elod Maros · Peter Balla · Gergo Kiszner · Ivett Teleki · Csaba Kovago · Tibor Krenacs

Received: 14 April 2014 / Revised: 10 June 2014 / Accepted: 11 June 2014 / Published online: 29 June 2014

Abstract In modulated electrohyperthermia (mEHT) the enrichment of electric field and the concomitant heat can selectively induce cell death in malignant tumors as a result of elevated glycolysis, lactate production (Warburg effect), and reduced electric impedance in cancer compared to normal tissues. Earlier, we showed in HT29 colorectal cancer xenografts that the mEHT-provoked programmed cell death was dominantly caspase independent and driven by apoptosis inducing factor activation. Using this model here, we studied the mEHT-related cell stress 0-, 1-, 4-, 8-, 14-, 24-, 48-, 72-, 120-, 168- and 216-h post-treatment by focusing on damage-associated molecular pattern (DAMP) signals. Significant cell death response upon mEHT treatment was accompanied by the early upregulation (4-h post-treatment) of heat shock protein (Hsp70 and Hsp90) mRNA levels. In situ, the treatment resulted in spatio-temporal occurrence of a DAMP protein signal sequence featured by the significant cytoplasmic to cell membrane translocation of calreticulin at 4 h, Hsp70 between 14 and 24 h and Hsp90 between 24- and 216-h post-treatment. The release of high-mobility group box1 protein (HMGB1) from tumor cell nuclei from 24-h post-treatment and its clearance from tumor cells by 48 h was also detected. Our results suggest that mEHT treatment can induce a DAMP-related signal sequence in colorectal cancer xenografts that may be relevant for promoting immunological cell death response, which need to be further tested in immune-competent animals.

Keywords Modulated electrohyperthermia · Damage-associated molecular pattern · Calreticulin · Heat shock protein · High-mobility group box1 protein

Gabor Andocs and Nora Meggyeshazi equally contributed to this work.

G. Andocs
Department of Radiological Sciences, Graduate School of Medicine and Pharmaceutical Sciences, University of Toyama, Toyama, Japan

N. Meggyeshazi · M. E. Maros · P. Balla · G. Kiszner · I. Teleki · T. Krenacs (✉)
1st Department of Pathology and Experimental Cancer Research, Semmelweis University, Ulloi ut 26. 1085, Budapest, Hungary
e-mail: krenacst@gmail.com

L. Balogh
"Frederic Joliot Curie" National Research Institute for Radiobiology and Radiohygiene, Budapest, Hungary

S. Spisak
MTA-SE Molecular Medicine Research Group, Budapest, Hungary

C. Kovago
Department of Pharmacology and Toxicology, Faculty of Veterinary Science, Szent Istvan University, Budapest, Hungary

T. Krenacs
MTA-SE Tumor Progression Research Group, Budapest, Hungary

Introduction

Modulated electrohyperthermia (mEHT) is a non-invasive local technique using capacitive coupled 13.56-MHz radiofrequency for targeted destruction of tumor cells (Andocs et al. 2009a) based on the elevated conductivity, permittivity, and current density in cancer compared to normal tissue (Andocs et al. 2009b; Blad and Baldetorp 1996; Blad et al. 1999; Fiorentini and Szasz 2006; Zou and Guo 2003). We have previously revealed that mEHT at <42 °C can dominantly induce a caspase-independent programmed cell death in HT29 colorectal cancer xenografts as a result of cell stress

synergistically induced by the electric field and heat (Andocs et al. 2009a; Meggyeshazi et al. 2014). Other groups have demonstrated that mild whole-body hyperthermia of tumors between ~38 and 42 °C can generate immunogenic host response (Frey et al. 2012; Mace et al. 2012) and local hyperthermia can cause heat shock protein (Hsp) 70 increment along with high-mobility group box 1 (HMGB1) protein release due to stress and necrosis (Frey et al. 2012; Multhoff et al. 2012; Schildkopf et al. 2010). These signs were suggestive of programmed cell death-related damage signals which may lead to immunogenic tumor cell death (ICD) (Garg et al. 2013).

The spatiotemporal appearance of the so-called damage-associated molecular pattern (DAMP) signals can promote the uptake of tumor antigens by antigen presenting cells and lead to ICD (D'Eliseo et al. 2013; Garg et al. 2012; Kepp et al. 2011; Ladoire et al. 2013; Scheffer et al. 2003; Ullrich et al. 2008). The danger signals combined with cancer antigens can stimulate the maturation of antigen presenting cells, which finally "cross prime" and activate anti-tumor T cell immunity (Kepp et al. 2011; Sachamitr and Fairchild 2012). The DAMP sequence, relevant to induce ICD in tumor cells, include the pre-apoptotic surface exposure of calreticulin, the surface appearance of heat shock proteins (Hsp70 and Hsp90) and ATP release at early apoptotic stages, followed by passive release of high-mobility group box 1 (HMGB1) as well as Hsp70 and Hsp90 at the late stages (D'Eliseo et al. 2013; Garg et al. 2010, 2012, 2013; Kepp et al. 2011; Ladoire et al. 2013; Martins et al. 2012). ICD is known to be provoked by massive cell stress in synergy with programmed cell death (D'Eliseo et al. 2013; Kepp et al. 2009; Krysko et al. 2013; Ladoire et al. 2013) using chemotherapeutic agents (doxorubicin, oxaliplatin, etc.) (Ladoire et al. 2013; Tesniere et al. 2010), cardiac glycosides (Menger et al. 2012), hypericin-based photodynamic therapy (Castano et al. 2006; Garg et al. 2012; Mroz et al. 2011) or capsaicin (D'Eliseo et al. 2013). It is of note, however, that these interventions can generate slightly different DAMP patterns (Garg et al. 2013; Kroemer et al. 2013).

This is a feasibility study to see if mEHT can provoke DAMP-related signals in our HT29 colorectal cancer xenograft model. Proving such effect can facilitate the testing of direct correlations between mEHT-induced DAMP signals and ICD in immune-competent animal models and would support the rationale of using mEHT as a supplemental therapy with chemotherapy, as it has already been used with benefit for treating recurrent breast cancer, glioblastoma multiforme, and colorectal cancer metastases to the liver, based mainly on empirical observations (Feyerabend et al. 2001; Fiorentini et al. 2006; Hager et al. 1999).

Material and methods

Animal model and treatment

Six to eight-week old Balb/c (nu/nu) mice were subcutaneously injected into both femoral regions with 0.1-ml suspension of 10^7/ml HT29 tumor cells, grown in DMEM + GlutaMAX, high-glucose (4.5 g/l) medium, as described before (Meggyeshazi et al. 2014). Local mEHT in the right leg of animals were delivered using plan-parallel electric condenser of the circuit in asymmetrical electrode arrangement on day-18 of tumor injection when symmetrical tumors measured ~1.5-cm diameter. A rectangular grounded (lower) aluminum electrode of 72.0 cm^2, kept at 37 °C during was below the animals and a 2.5 cm^2 round copper–silver–tin-coated flexible textile electrode (Lorix Ltd. Bajna, Hungary) was overlaid on the tumors, which were cooled under control using a wet pad. Electromagnetic heating was generated by capacitive coupled, amplitude-modulated 13.56 MHz radiofrequency (LabEHY, Oncotherm Kft, Paty, Hungary).

Under 100 mg/kg ketamine and 10 mg/kg xylazine anesthesia, 33 animals were treated with a single shot of mEHT for 30 min using 4-W average power. Intratumoral temperature was kept at ~42 °C (±0.5 °C) as measured with optical sensors (Luxtron FOT Lab Kit, LumaSense Technologies, Inc. CA). The subcutaneous temperature under the electrode was kept at ~40 °C and the rectal temperature at ~37 °C. Samples were collected 0, 1, 4, 8, 14, 24, 48, 72, 120, 168, and 216 h after treatment from three mice in each group. Also, five tumor implanted sham-treated animals were sacrificed 24- and 72-h post-treatment. One half of the excised tumor was fresh frozen in liquid nitrogen and kept at −80 °C. The other half was fixed in 10 % formalin, dehydrated, and embedded into paraffin wax (FFPE). The study was approved by the Governmental Ethical Committee under No. 22.1/609/001/2010.

mRNA expression microarray analysis

Total RNA isolation and RNA quality control

Frozen tissue sections were prepared from the 4-h post-treatment treated and untreated samples together with the 24-h sham-treated controls. Total RNA was extracted by Roche MagNA Pure LC RNA Isolation Tissue Kit (Roche, Basel, Switzerland). RNA concentration was measured by NanoDrop instrument (Thermo Scientific, Rockford, IL, USA). The quality of the nucleic acid was determined with microcapillary electrophoresis system using Agilent Bioanalyzer 6000 Pico LabChip kit (Aligent

Technologies, Santa Clara, CA, USA). With RNA integrity number above 7 (RIN >7) 100 ng total RNA from each sample were mixed and 250 ng pooled total RNA was amplified and labeled in each group.

Microarray analysis

The recommendation of minimum information about a microarray experiment (MIAME) guideline was followed (Brazma et al. 2001). Amplification and labeling of the transcripts was performed by using Affymetrix 3′ IVT Express Kit (Affymetrix, Santa Clara, CA, USA). Samples were hybridized on HGU133 Plus 2.0 arrays (Affymetrix) at 45 °C for 16 h. The microarrays were washed and stained on Fluidics Station 450 device (Affymetrix) using the vendors kit with the FS450_001 wash protocol. Fluorescent signals were detected by Gene Chip Scanner 3000 (Affymetrix) following the antibody-based signal amplification with streptavidin–phycoerythrin according to manufacturer's instructions.

From the CEL files, quality control and RNA digestion plots were generated in R-environment using the Bioconductor system. The differentially expressed genes between the analyzed sample groups were determined by significance analysis of microarrays (SAM) at the significance level of $p<0.05$. Feature selections were done according to the log2FC (log2 fold change) values to select at least twofold up/downregulated genes.

The row datasets mRNA expression in mEHT-treated HT29 xenografts are available in the Gene Expression Omnibus databank for further analysis (http://www.ncbi.nlm.nih.gov/geo/), series accession number: GSE58750.

Apoptosis array

Proteins were isolated from the frozen samples using extraction buffer (20-mM Tris, 2-mM EDTA, 150-mM NaCl, 1 % Triton-X100, 10 μl/ml phosphatase inhibitor and 5 μl/ml proteinase inhibitors) for 30 min on ice, followed by centrifugation at 15,000 rpm at 4 °C for 15 min. Lysates were prepared from the 8-, 14-, and 24-h-treated and 24-h sham-treated samples and the protein concentration set up for 100 μg/μl based on the Bradford assay. The expression of 35 apoptosis-related proteins was tested using a nitrocellulose membrane Proteome Profiler™ Human Apoptosis Array Kit array (R&D, Minneapolis, MN). Arrays were incubated on a shaker with 250 μl of 1,200 μg/ml protein lysates at 4 °C overnight, then with biotinylated anti-human IgG for 60 min and streptavidin-horseradish peroxidase (HRP) conjugate for 30 min and visualized using a chemiluminescence ECL kit (SuperSignal® West Pico Chemiluminescent Kit; Thermo Scientific, Rockford, IL) for 10-min in a Kodak Image Station 4,000 mm (Rochester, NY). For semi-quantitative analysis, the ImageJ 1.45 software was used (http://rsbweb.nih.gov/ij/).

Immunohistochemistry

Tissue microarrays (TMA) including three cores of 2-mm diameter from standard areas, two from the edges of degraded and intact tumor border, and one from the degraded center in each donor block were created from the archived tissues using the semi-automated TMA Master (3DHISTECH Ltd., Budapest, Hungary). For antigen retrieval, dewaxed and rehydrated TMA slides of 4-μm thickness were heated at ~100 °C for 40 min using a microwave oven (Whirlpool, Benton Harbor, MI) either with citrate buffer pH 0.6 (0.01-M sodium citrate–citric acid; for HMGB1) or with Tris-EDTA (TE) buffer pH 9.0 (0.1-M Trisbase and 0.01-M ethylenediaminetetraacetic acid for all other antibodies) followed by bovine serum albumin (BSA)–azide (5 %, Sigma-Aldrich, St. Luis, MO) treatment for 20 min. Then, sections were incubated in a humidity chamber at room temperature for 16 h using the following antibodies: polyclonal rabbit anti-human calreticulin (1:100), Hsp70 (1:50), Hsp90 (1:100), and HMGB1 (1:200) (all from Cell Signaling, Danvers, MA). These were then detected using Alexa Fluor 546 (orange-red) coupled anti-rabbit Ig (1:200) for 90 min. For slide washing, 0.1-M tris-buffered saline (pH 7.4) was used. Cell nuclei were stained blue using 4′,6-diamidino-2-phenylindole (DAPI) and cell membranes were highlighted using a wheat germ agglutinin alexa fluor 488 conjugate (1:200). All fluorescent probes were from Invitrogen/Molecular Probes. Between incubation steps the slides were washed in 0.1-M Tris-buffered saline (pH 7.4) buffer.

Evaluation methods

Biomarker expression revealed by immunofluorescence was evaluated using image (color, intensity, and size) segmentation-based software HistoQuant (3DHISTECH). Three to five representative annotations per tumor section involving >1,000 cells each were tested. Relative mask area (rMA) was calculated by dividing the stained area with the whole annotation area except for calreticulin staining, where membrane positive cells were counted in 10 fields of views (FOV) in each core at ×100 magnification. For analyzing protein expression data related to a single time point that followed normal distribution, the independent T test was used. For time series data analysis, the Friedman test was used

followed by the Wilcoxon post hoc test. The results were significant at $p<0.05$.

Results

Messenger RNA expression was measured from pooled samples of the 4 h treated, 4 h untreated, and 24 h sham-treated tumors, respectively. Modulated electrohyperthermia (EHT) treatment induced significant up- or down-regulation of 48 transcripts of 39 genes compared to controls. Members of the heat shock protein 70 family including HSPA1A, HSPA1B, HSPA4, HSPA6, and HSPA8, and their co-chaperones Hsp40 (DNAJB1 and DNAJB4) and Bag3 became up-regulated. Hsp90 alpha (HSP90AA1) and Hsp60 (HSPD1) gene transcripts were also elevated upon mEHT treatment (Fig. 1).

Apoptosis protein array testing of pooled lysates of 8-, 14-, 24 h-treated and 24 h sham-treated tumors also showed a twofold increase of Hsp70 levels (1.92±0.027) at 8 h post-treatment (Fig. 2a).

Modulated EHT-related tissue damage was characterized by a progressive destruction of the central tumor area from 24 h post-treatment on surrounded by an external rim of intact-looking tumor cells and a transitional zone in between these two. Immunofluorescence analysis revealed significantly elevated expression of Hsp70 in the treated compared to the untreated group (χ^2 (19)=54.634, $p<0.05$). The post hoc test confirmed the significant difference at 14-, 24-, 72-, and 120-h post-treatment with a transitional decrement at 48 h. At 14 h post-treatment Hsp70 protein was mainly associated to the cytoplasmic membrane in the treated xenografts. At later (72–120 h) stages Hsp70 upregulation was observed only in the transient zone between the morphologically intact and dead tumor areas (Fig. 2b, c). Also, significantly increased Hsp90 levels were detected (χ^2 (21)=83.559, $p<0.05$) in the treated compared to the untreated groups, which was confirmed with the post hoc test at 24-, 48-, 72-, 120-, 168- and 216 h after mEHT treatment (Fig. 3). Hsp90 translocated to the cytoplasm membrane only at later time points (168- and 216 h post-treatment). In contrast to Hsp70, Hsp90 levels showed continuous elevation in the treated tumor cells between 24 and 216 h. Furthermore, the early accumulation of calreticulin to the cell membrane was observed at 4 h ($p=0.001$) post-treatment (Fig. 4).

HMGB1 protein was detected in cell nuclei up to 14 h, both in the treated and in the untreated samples, followed by cytoplasmic translocation at 24 h in the treated xenografts. HMGB1 immunofluorescence disappeared 48 h post-treatment in the damaged central areas of the treated tumors

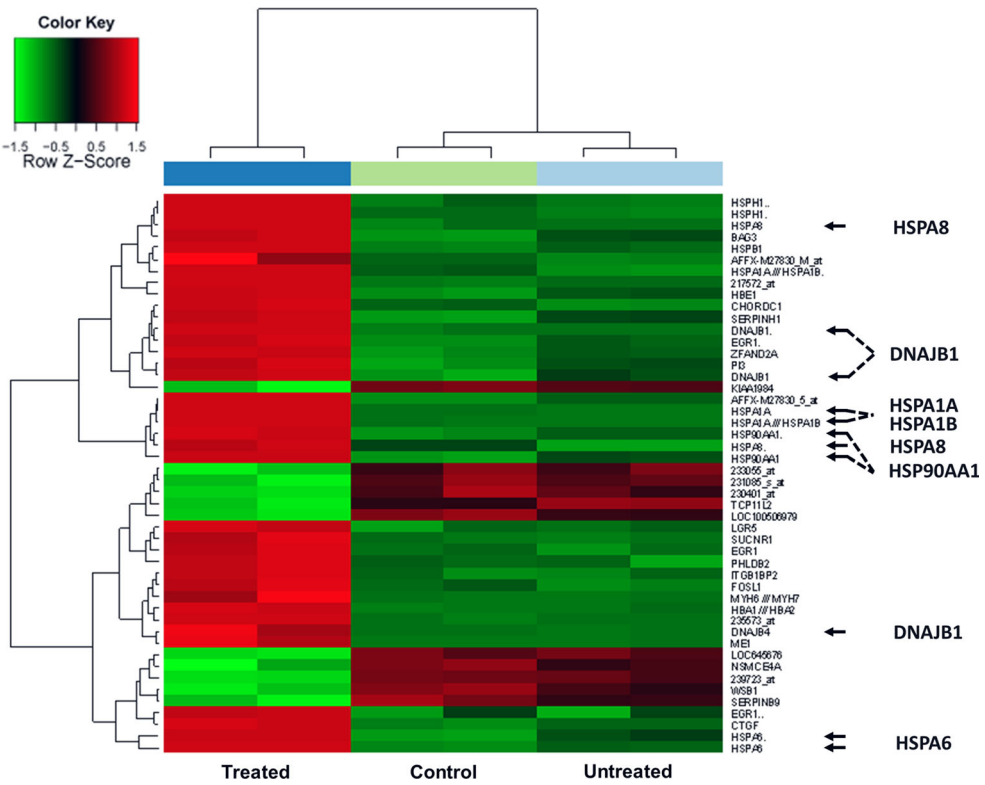

Fig. 1 Heat map on gene expression summarizing transcripts showing significantly differential expression 4 h after mEHT treatment of HT29 colon cancer xenografts. *Arrows* highlight the elevated expression (*red boxes*) of heat shock protein genes from the Hsp70, Hsp40, Hsp90, and Hsp60 families in the treated samples (*left column*) compared either to sham treated (*middle*) and untreated samples (*right*)

while still prevailed in the untreated controls. In the treated tumors nuclear HMGB1 protein was significantly lost (χ^2 (19)=64.657, $p<0.05$) compared to the untreated group, as it was also supported by the post-hoc test at each time point between 24 and 216 h post-treatment (Fig. 5).

Discussion

Earlier, we detected mEHT-induced significant tumor cell destruction as a result of the synergistic effects of electric field and heat (Andocs et al. 2009a). This stress caused caspase-independent programmed cell death through Bax-mediated mitochondrial pore formation and the concomitant release of cytochrome c and the activation of apoptotic inducing factor (AIF) (Meggyeshazi et al. 2014). Here, we detected a characteristic DAMP signal sequence in HT29 colorectal cancer xenografts upon mEHT treatment, which can potentially induce an ICD response as it has been demonstrated in diverse tumor models (D'Eliseo et al. 2013; Garg et al. 2012).

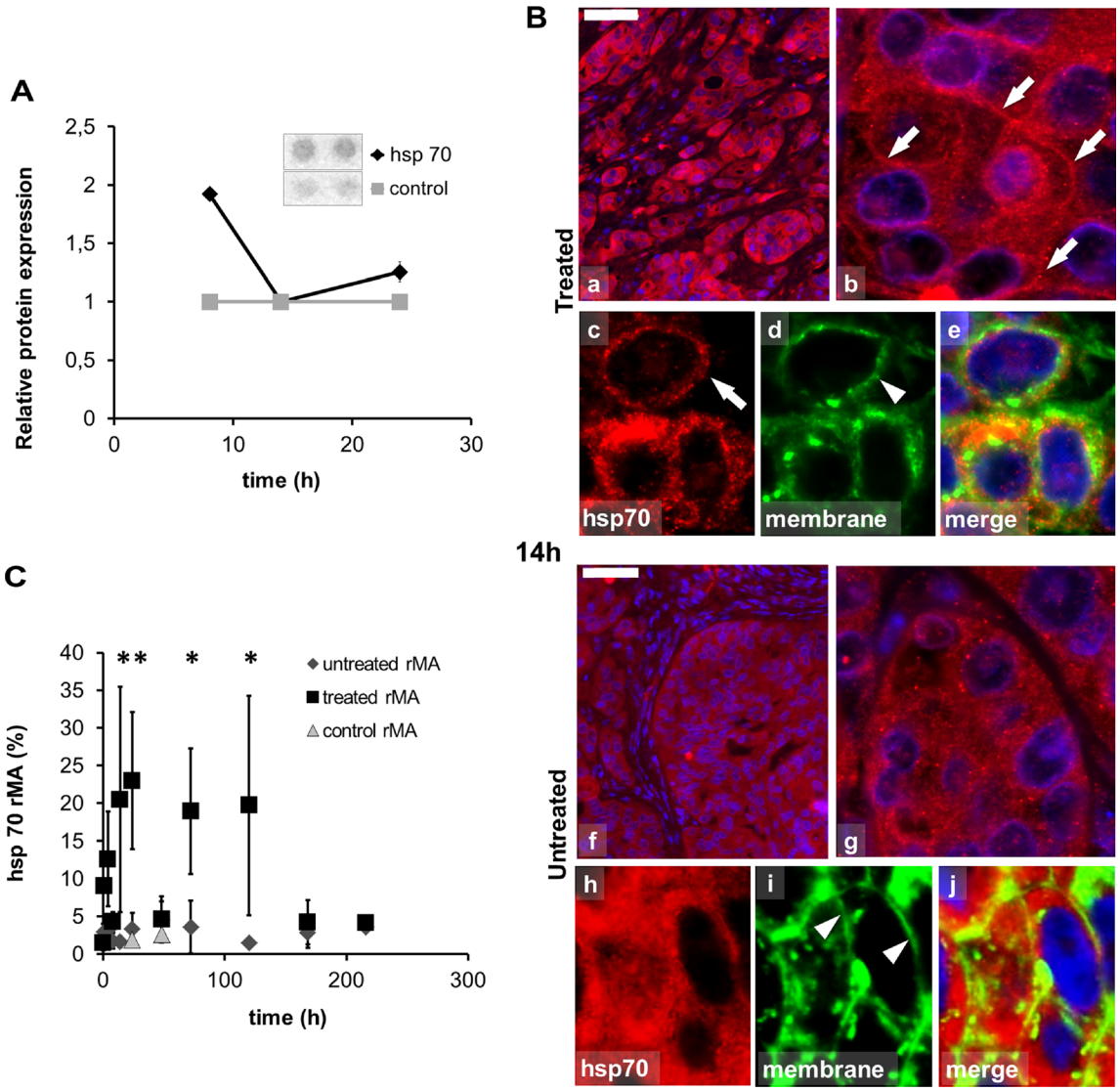

Fig. 2 Abundance and localization of heat shock protein 70 (Hsp70) in colorectal cancer xenografts measured with apoptosis protein array and immunofluorescence (Alexa 564, *red*). **a** Pooled tissue samples reveal elevated Hsp70 levels in apoptosis protein array at 8 h with no change at 14 and 24 h due to inhomogeneity of the tissue at these time points. **b** Hsp70 immunofluorescence (Alexa 564, *red*), in 14-h post-mEHT treated (*a–e*) and untreated (*f–j*) tumor cells also immunoreacted with wheat germ agglutinin (Alexa 488, *green*) and DAPI to stain nuclei. In 14 h post-mEHT-treated tumor cells Hsp70 immunofluorescence is predominately in cell membranes (*arrows*) as indicated by the wheat germ agglutinin reactivity (*arrowheads*). In the untreated tumor cells Hsp70 immunofluorescence is predominately cytoplasmic. Scale bar=80 μm in *a* and *f*, 10 μm in *b* and *g*, and 5 μm in *c*, *d*, *e*, *h*, *i*, and *j*. **c** Semi-quantitative image analysis of immunofluorescence confirms significant elevation of Hsp70 levels both between 14–24 h and 72–120 h post-treatment (*$p<0.05$) with a decline at 48 h (*rMA* relative mask area)

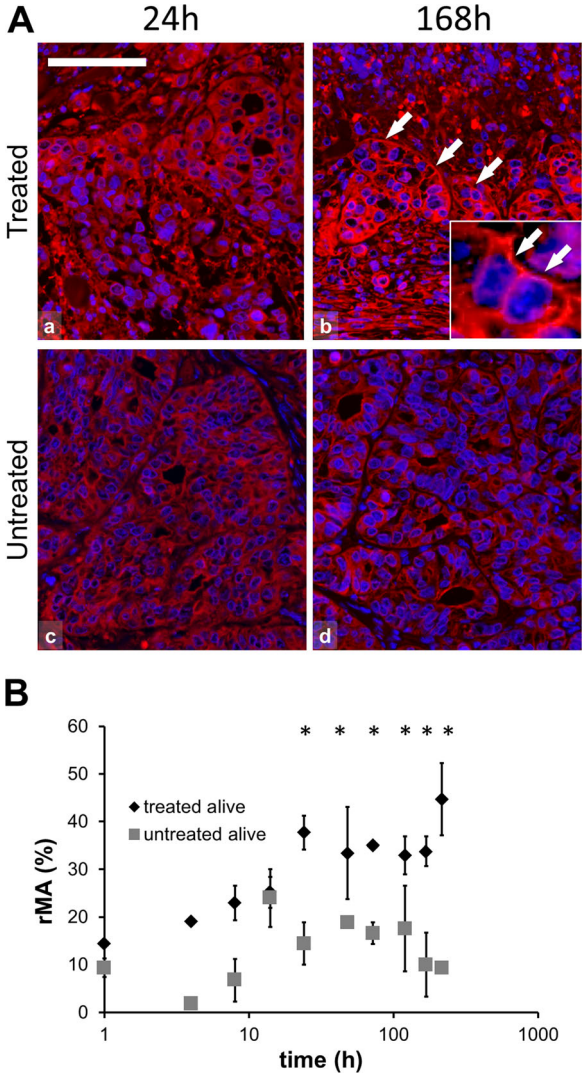

Fig. 3 Hsp90 immunofluorescence (Alexa 564, *red*) and semi-quantitative analysis of heat shock protein 90 (Hsp90) in post-mEHT treated and untreated colorectal cancer xenografts. **a** Hsp90 immunofluorescence is predominately cytoplasmic at 24 h (*a*) and associated with cell membranes at 168 h post-mEHT (*b*; *arrows*), and as shown in the *inset*. Hsp90 immunofluorescence is less apparent at 24 h (*c*) and at 168 h (*d*) in untreated tumor cells. Cell nuclei are stained blue (DAPI). *Scale bar*= 60 μm in all and 20 μm in the inset. **b** Graph showing significant increase of Hsp90 protein between 24 and 216 h in the treated compared to the untreated tumor cells in the morphologically intact tumor areas (*$p<0.05$) (*rMA* relative mask area)

ICD requires antigen linked spatiotemporal DAMP signals including the cell surface translocation of calreticulin and heat shock proteins (Hsp70 and Hsp90) followed by ATP liberation and the passive release of HMGB1 protein from the nucleus during the late apoptotic stage (D'Eliseo et al. 2013; Garg et al. 2012, 2013; Kepp et al. 2011; Kroemer et al. 2013; Krysko et al. 2013; Ladoire et al. 2013).

Calreticulin, as a chaperone in the endoplasmic reticulum (ER), interacts with ERp57 and calnexin and supports proper protein folding and modulates calcium signaling and homeostasis (Ladoire et al. 2013). In tumor cell death-related immunogenicity, calreticulin can translocate into lipid rafts of the plasma membrane where it is called as ecto-calreticulin and serves as an early "eat me" signal for antigen presenting dendritic cells (Garg et al. 2013; Obeid et al. 2007). Upon anthracyclin and ionizing radiation therapy, detection of ecto-calreticulin was one of the first molecular events of ICD-related DAMPs, occurring before any morphological signs of apoptosis (Ladoire et al. 2013). In line with this, we detected ecto-calreticulin as early as 4 h after mEHT treatment also preceding programmed cell death signals, which later we saw first at 8-h post-treatment in the same HT29 xenograft model (Meggyeshazi et al. 2014).

Heat shock proteins are a family of conserved chaperones induced by cell stress including oxidative stress, irradiation, chemotherapeutic drugs, and heat and electromagnetic field (Blank and Goodman 2009; Horvath and Vigh 2010; Robert 2003). Tumors frequently show elevated Hsp70 levels (Multhoff and Hightower 2011). In the cytoplasm, overexpressed Hsp70 can inhibit apoptosis and act as a cytoprotector (Horvath and Vigh 2010) maintaining protein homeostasis (Gehrmann et al. 2008). However, treatments using oxaliplatin, γ-radiation, anthracyclines, epidermal growth factor receptor-specific antibody or hypericin-based photodynamic therapy can trigger the cell membrane accumulation of heat shock proteins (Kroemer et al. 2013; Krysko et al. 2013) as a part of the spatiotemporal DAMP signals and promote anti-tumor T cell response (Garg et al. 2013). Besides the immunogenicity of cell membrane Hsp70 (Gehrmann et al. 2008), extracellular heat shock proteins can directly boost the innate immune response (Calderwood et al. 2007; Multhoff and Hightower 2011). In this study, mEHT-related cell membrane accumulation of Hsp70 was observed from 14 h post-treatment with two peaks at 24 h and 72 h with a decrement at 48 h. The second peak was most probably associated with soluble factors released from damaged cells. Similar double peaks in Hsp70 levels (at 12 and 72 h) were seen by others in bladder cancer cells treated with capsaicin-inducing ICD through a DAMP sequence (D'Eliseo et al. 2013). On the other hand, cell membrane Hsp70 was also linked with the protection of membrane integrity under stress conditions (Horvath and Vigh 2010). Therefore, in tumor therapy, cell surface Hsp70 positivity has been associated both with negative prognosis, e.g., in lower rectal carcinomas and in squamous cell carcinoma of the lung (Gehrmann et al. 2008; Pfister et al. 2007) and also, with improved outcome, e.g., in gastric and colon carcinomas (Pfister et al.

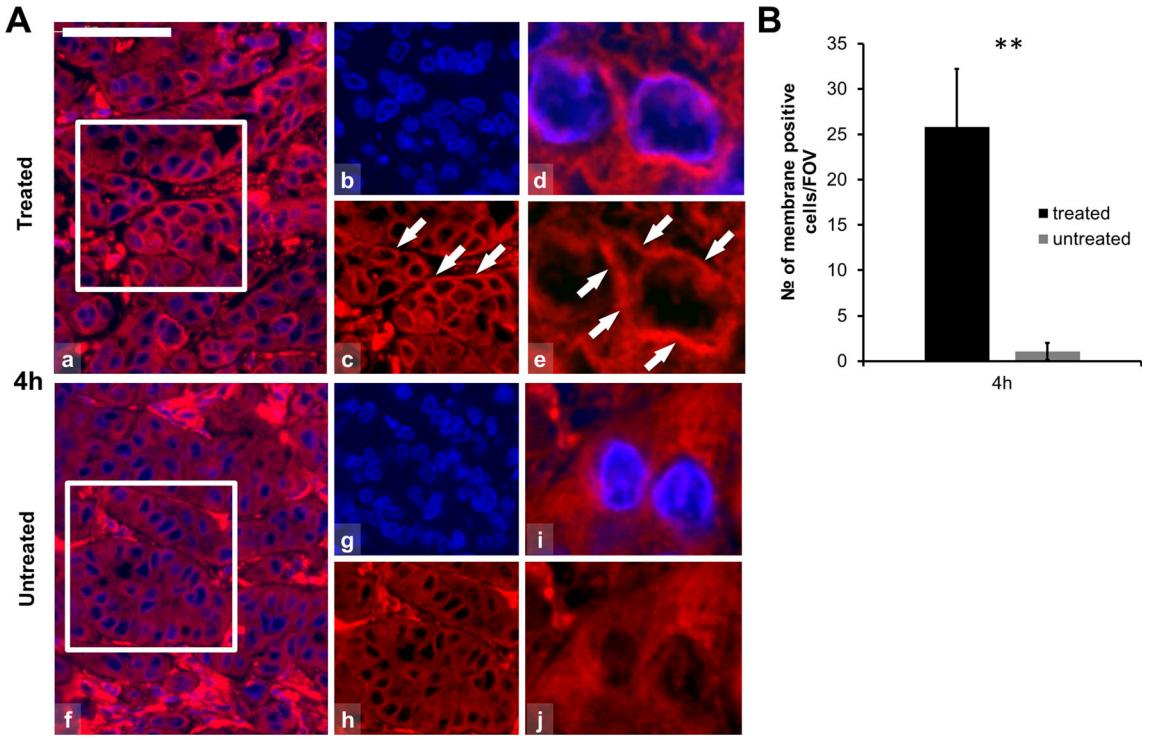

Fig. 4 Calreticulin immunofluorescence (Alexa 564, *red*) and semi-quantitative analysis of calreticulin in post-mEHT treated and untreated colorectal cancer xenografts. **a** Calreticulin immunofluorescence is localized to the cell membranes 4 h post-mEHT (*arrows*; *a–e*) before any morphological or molecular sign of programmed cell death. Calreticulin immunofluorescence is diffuse and cytoplasmic in untreated tumor cells (*f–j*). Cells nuclei are stained blue (DAPI). *Scale bar*=60 μm in *a*, *b*, *c*, *f*, *g*, and *h* and 10 μm in *d*, *e*, *i*, and *j*. **b** Graph showing the mean number of cytoplasmic membrane positive cells counted at ×100 magnification in 10 fields of views (FOV) of five parallel samples. Elevation of calreticulin cell membrane immunofluorescence is highly significant (**$p<0.01$) in 4 h post-mEHT treated compared to untreated tumor cells (*FOV* field of view)

2007). This latter is in line with our findings in HT29 colon cancer xenografts where mEHT treatment resulted in tumor cell death.

Membrane associated Hsp90 can also be a member of DAMP sequence linked to ICD, e.g., upon epidermal growth factor receptor antibody therapy and hypericin-based photodynamic therapy (Garg et al. 2013). Similar to that found by others upon hypericin phototherapy and capsaicin-induced DAMP signals, we also detected the cell membrane accumulation and late apoptotic release of Hsp90 from 168 h post-mEHT treatment (D'Eliseo et al. 2013; Garg et al. 2013).

HMGB1 represents a late signal of ICD with diverse roles. In the nucleus, it acts as a non-histone chromatin binding protein interacting with the minor groove of DNA and regulatory molecules such as p53, NF-κB, and steroid hormone receptors (Guo et al. 2013; Kepp et al. 2011; Ladoire et al. 2013). Upon cell stress, HMGB1 is released either from necrotic or apoptotic cells (D'Eliseo et al. 2013). Extracellular HMGB1 can be a cytokine-like activator of macrophages, a chemotactant for neutrophils and a promoter of dendritic cell maturation through toll-like receptors (TLR2/4) (Guo et al. 2013). However, epigenetic and posttranslational modifications may attenuate the pro-inflammatory activity of HMGB1 (Guo et al. 2013). We detected the cytoplasmic release of HMGB1 protein at 24 h and its clearance from mEHT treated carcinoma cells by 48-h post-treatment, which has the potential to contribute both to the innate and T cell immune responses.

Elevated glycolysis in tumor cells, known as the Warburg effect, can increase permittivity and conductivity (Andocs et al. 2009b; Blad and Baldetorp 1996; Blad et al. 1999; Fiorentini and Szasz 2006; Zou and Guo 2003), which support mEHT to selectively damage tumor cells (Andocs et al. 2009a) without affecting normal tissues. The electric field and heat can induce cellular stress signals (Balogh et al. 2013) leading to Bax-mediated mitochondrial dysfunction, pore formation, and programmed cell death (Meggyeshazi et al. 2014). The benefit of mEHT that it can locally induce DAMP signals without the systemic damage of immune cells caused by traditional ICD inducer chemotherapies, especially if steroids are also part of the therapy (Garg et al. 2013).

The ultimate outcome of immune response to cancer cell death is rather complex and context dependent. Cell

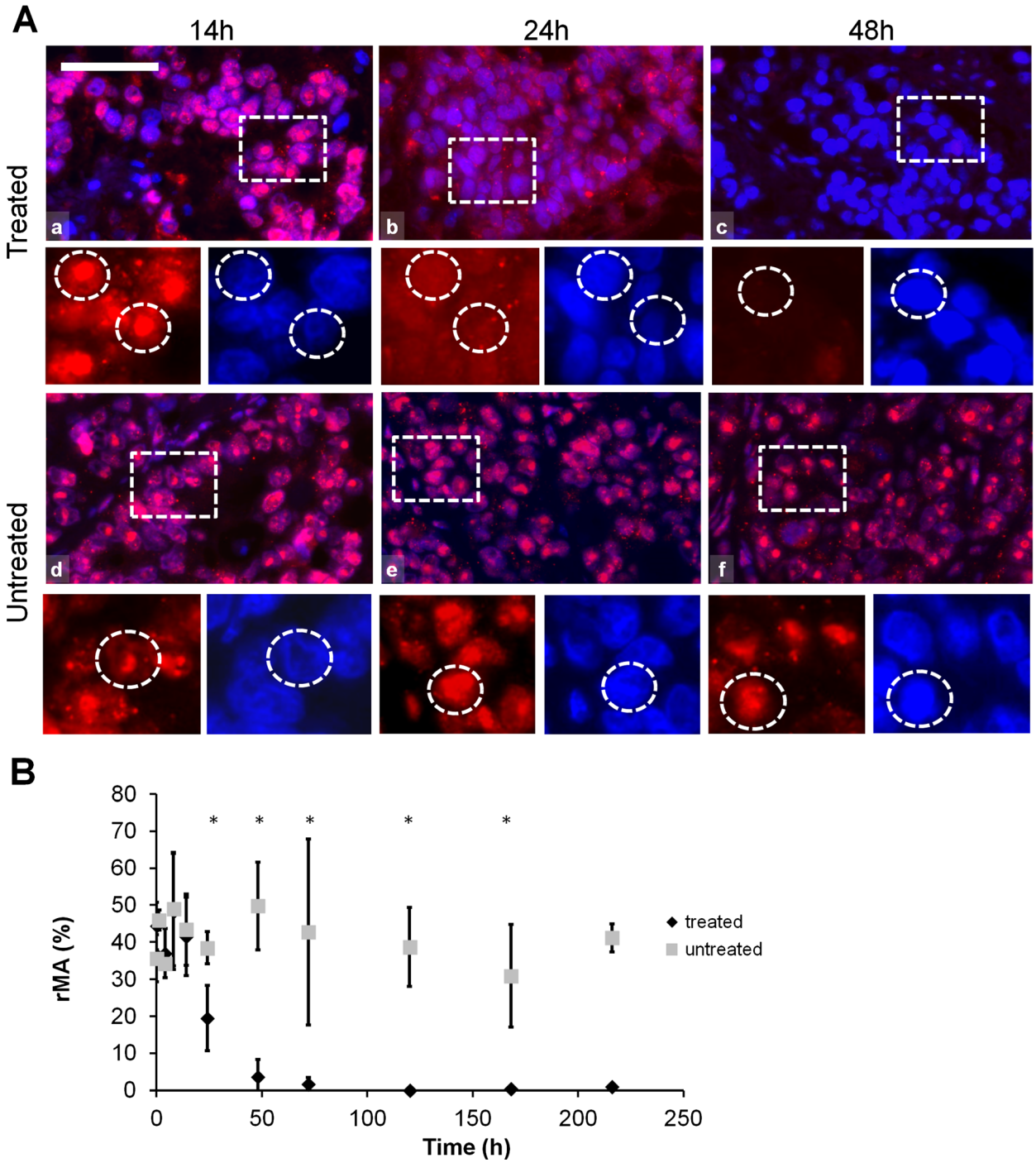

Fig. 5 HMGB1 immunofluorescence (Alexa 564, *red*) and semi-quantitative analysis of HMGB1 post-mEHT treated and untreated colorectal cancer xenografts. **a** HMGB1 immunofluorescence shows normal nuclear localization up to 14 h post-mEHT treated (*a*) and untreated (*d*) tumor cells. HMGB1 immunofluorescence is diffuse and diminished in 24 h and not evident in 48 h post-mEHT treated (*b* and *c*, respectively) tumor cells but not changed in 24 and 48 h untreated (*e* and *f*, respectively) tumor cells. *Boxes* show the location of the high-magnification *insets*. *Circles* in the insets show the location of nuclei. *Scale bar*=60 μm in *a*, *b*, *c*, *d*, *e* and *f*, and 25 μm in all insets. **b** Semi-quantitative analysis highlights significant reduction of HMGB1 immunofluorescence between 48 and 216 h post-mEHT treated compared to untreated tumor cells (*$p<0.05$) (*rMA* relative mask area)

death is influenced by the type and localization/microenvironment of cancer cells, the cell death pathways activated, the type of immune cells interacting with the cancer, and the efficiency of the recognition of cancer antigens (Garg et al. 2013). Though our results cannot be linked directly to ICD, detection of DAMP signals in colon cancer supports the feasibility of testing if mEHT treatment can directly promote ICD in tumors raised in immune competent animals.

In conclusion, based on sporadic observations of earlier in vitro studies of local hyperthermia (Frey et al. 2012; Mantel et al. 2010; Schildkopf et al. 2010), here, we showed, in vivo, that mEHT induced tumor cell stress can generate the spatiotemporal sequence of DAMP signals in colorectal cancer without any additional genetic or pharmaceutical intervention. Our data suggest that mEHT can be a potential local inducer of ICD, without a systemic interference with immune functions, which need to be investigated further in immune competent animal models.

Acknowledgments The authors are utterly grateful to Edith Parsch, Renata Papp, and Sandor Kiss for their technical assistance. This work was supported by TET_10-1-2011-0914 grant in Hungary.

References

Andocs G, Renner H, Balogh L, Fonyad L, Jakab C, Szasz A (2009a) Strong synergy of heat and modulated electromagnetic field in tumor cell killing. Strahlenther Onkol Organ Dtsch Rontgengesellschaft 185:120–126. doi:10.1007/s00066-009-1903-1

Andocs G, Szasz O, Szasz A (2009b) Oncothermia treatment of cancer: from the laboratory to clinic. Electromagn Biol Med 28:148–165. doi:10.1080/15368370902724633

Balogh G et al (2013) Key role of lipids in heat stress management. FEBS Lett 587:1970–1980. doi:10.1016/j.febslet.2013.05.016

Blad B, Baldetorp B (1996) Impedance spectra of tumour tissue in comparison with normal tissue. A possible clinical application for electrical impedance tomography. Physiol Meas 17:A105–A115. doi:10.1088/0967-3334/17/4a/015

Blad B, Wendel P, Jonsson M, Lindstrom K (1999) An electrical impedance index to distinguish between normal and cancerous tissues. J Med Eng Technol 23:57–62. doi:10.1080/030919099294294

Blank M, Goodman R (2009) Electromagnetic fields stress living cells. Pathophysiol Off J Int Soc Pathophysiol/ISP 16:71–78. doi:10.1016/j.pathophys.2009.01.006

Brazma A et al (2001) Minimum information about a microarray experiment (MIAME)—toward standards for microarray data. Nat Genet 29:365–371

Calderwood SK, Mambula SS, Gray PJ Jr (2007) Extracellular heat shock proteins in cell signaling and immunity. Ann N Y Acad Sci 1113:28–39. doi:10.1196/annals.1391.019

Castano AP, Mroz P, Hamblin MR (2006) Photodynamic therapy and anti-tumour immunity. Nat Rev Cancer 6:535–545. doi:10.1038/nrc1894

D'Eliseo D, Manzi L, Velotti F (2013) Capsaicin as an inducer of damage-associated molecular patterns (DAMPs) of immunogenic cell death (ICD) in human bladder cancer cells. Cell Stress Chaperones. doi:10.1007/s12192-013-0422-2

Feyerabend T, Wiedemann GJ, Jager B, Vesely H, Mahlmann B, Richter E (2001) Local hyperthermia, radiation, and chemotherapy in recurrent breast cancer is feasible and effective except for inflammatory disease. Int J Radiat Oncol Biol Phys 49:1317–1325

Fiorentini G, Szasz A (2006) Hyperthermia today: electric energy, a new opportunity in cancer treatment. J Cancer Res Ther 2:41–46

Fiorentini G, Giovanis P, Rossi S, Dentico P, Paola R, Turrisi G, Bernardeschi P (2006) A phase II clinical study on relapsed malignant gliomas treated with electro-hyperthermia. In vivo (Athens, Greece) 20:721–724

Frey B et al (2012) Old and new facts about hyperthermia-induced modulations of the immune system. Int J Hyperther Off J Eur Soc Hyperther Oncol N Am Hyperther Group 28:528–542. doi:10.3109/02656736.2012.677933

Garg AD, Nowis D, Golab J, Vandenabeele P, Krysko DV, Agostinis P (2010) Immunogenic cell death, DAMPs and anticancer therapeutics: an emerging amalgamation. Biochim Biophys Acta 1805:53–71. doi:10.1016/j.bbcan.2009.08.003

Garg AD, Krysko DV, Vandenabeele P, Agostinis P (2012) Hypericin-based photodynamic therapy induces surface exposure of damage-associated molecular patterns like HSP70 and calreticulin. Cancer Immunol Immunother CII 61:215–221

Garg AD, Martin S, Golab J, Agostinis P (2013) Danger signalling during cancer cell death: origins, plasticity and regulation. Cell Death Differ. doi:10.1038/cdd.2013.48

Gehrmann M, Radons J, Molls M, Multhoff G (2008) The therapeutic implications of clinically applied modifiers of heat shock protein 70 (Hsp70) expression by tumor cells. Cell Stress Chaperones 13:1–10. doi:10.1007/s12192-007-0006-0

Guo ZS, Liu Z, Bartlett DL, Tang D, Lotze MT (2013) Life after death: targeting high mobility group box 1 in emergent cancer therapies. Am J Cancer Res 3:1–20

Hager ED, Dziambor H, Hohmann D, Gallenbeck D, Stephan M, Popa C (1999) Deep hyperthermia with radiofrequencies in patients with liver metastases from colorectal cancer. Anticancer Res 19:3403–3408

Horvath I, Vigh L (2010) Cell biology: stability in times of stress. Nature 463:436–438. doi:10.1038/463436a

Kepp O, Tesniere A, Schlemmer F, Michaud M, Senovilla L, Zitvogel L, Kroemer G (2009) Immunogenic cell death modalities and their impact on cancer treatment. Apoptosis Int J Program Cell Death 14:364–375. doi:10.1007/s10495-008-0303-9

Kepp O et al (2011) Molecular determinants of immunogenic cell death elicited by anticancer chemotherapy. Cancer Metastasis Rev 30:61–69. doi:10.1007/s10555-011-9273-4

Kroemer G, Galluzzi L, Kepp O, Zitvogel L (2013) Immunogenic cell death in cancer therapy. Annu Rev Immunol 31:51–72. doi:10.1146/annurev-immunol-032712-100008

Krysko O, Love Aaes T, Bachert C, Vandenabeele P, Krysko DV (2013) Many faces of DAMPs in cancer therapy. Cell Death Dis 4:e631. doi:10.1038/cddis.2013.156

Ladoire S et al (2013) Cell-death-associated molecular patterns as determinants of cancer immunogenicity. Antioxid Redox Signal. doi:10.1089/ars.2012.5133

Mace TA, Zhong L, Kokolus KM, Repasky EA (2012) Effector CD8+ T cell IFN-gamma production and cytotoxicity are enhanced by mild hyperthermia. Int J Hyperther Off J Eur Soc Hyperther Oncol N Am Hyperther Group 28:9–18. doi:10.3109/02656736.2011.616182

Mantel F et al (2010) Combination of ionising irradiation and hyperthermia activates programmed apoptotic and necrotic cell death pathways in human colorectal carcinoma cells. Strahlenther Onkol Organ Dtsch Rontgengesellschaft 186:587–599. doi:10.1007/s00066-010-2154-x

Martins I et al (2012) Premortem autophagy determines the immunogenicity of chemotherapy-induced cancer cell death. Autophagy 8:413–415. doi:10.4161/auto.19009

Meggyeshazi N et al (2014) DNA fragmentation and caspase-independent programmed cell death by modulated electrohyperthermia. Strahlenther Onkol Organ Dtsch Rontgengesellschaft. doi:10.1007/s00066-014-0617-1

Menger L et al (2012) Cardiac glycosides exert anticancer effects by inducing immunogenic cell death. Sci Transl Med 4:143ra199. doi:10.1126/scitranslmed.3003807

Mroz P, Hashmi JT, Huang YY, Lange N, Hamblin MR (2011) Stimulation of anti-tumor immunity by photodynamic therapy. Expert Rev Clin Immunol 7:75–91. doi:10.1586/eci.10.81

Multhoff G, Hightower LE (2011) Distinguishing integral and receptor-bound heat shock protein 70 (Hsp70) on the cell surface by Hsp70-specific antibodies. Cell Stress Chaperones 16:251–255. doi:10.1007/s12192-010-0247-1

Multhoff G, Gaipl US, Niedermann G (2012) The role of radiotherapy in the induction of antitumor immune responses. Strahlenther Onkol Organ Dtsch Rontgengesellschaft 188(Suppl 3):312–315. doi:10.1007/s00066-012-0206-0

Obeid M et al (2007) Calreticulin exposure dictates the immunogenicity of cancer cell death. Nat Med 13:54–61. doi:10.1038/nm1523

Pfister K et al (2007) Patient survival by Hsp70 membrane phenotype: association with different routes of metastasis. Cancer 110:926–935

Robert J (2003) Evolution of heat shock protein and immunity. Dev Comp Immunol 27:449–464. doi:10.1016/S0145-305X(02)00160-X

Sachamitr P, Fairchild PJ (2012) Cross presentation of antigen by dendritic cells: mechanisms and implications for immunotherapy. Expert Rev Clin Immunol 8:547–555. doi:10.1586/eci.12.45

Scheffer SR et al (2003) Apoptotic, but not necrotic, tumor cell vaccines induce a potent immune response in vivo. Int J Cancer 103:205–211. doi:10.1002/ijc.10777

Schildkopf P et al (2010) Application of hyperthermia in addition to ionizing irradiation fosters necrotic cell death and HMGB1 release of colorectal tumor cells. Biochem Biophys Res Commun 391:1014–1020

Tesniere A et al (2010) Immunogenic death of colon cancer cells treated with oxaliplatin. Oncogene 29:482–491. doi:10.1038/onc.2009.356

Ullrich E, Bonmort M, Mignot G, Kroemer G, Zitvogel L (2008) Tumor stress, cell death and the ensuing immune response. Cell Death Differ 15:21–28

Zou Y, Guo Z (2003) A review of electrical impedance techniques for breast cancer detection. Med Eng Phys 25:79–90. doi:10.1016/s1350-4533(02)00194-7